Evaluation of the mixing performance in a planar passive micromixer with T micromixer with square chamber mixing units (SAR)

Attar, Hani; Zekry, Rahma S.; Sharfo, Samer M.; Deif, Mohanad A.; Hafez, Mohamed; Solyman, Ahmad

Published in:
2023 2nd International Engineering Conference on Electrical, Energy, and Artificial Intelligence (EICEEAI)

DOI:
10.1109/EICEEAI60672.2023.10590187

Publication date:
2024

Document Version
Author accepted manuscript

Evaluation of The Mixing Performance in a Planar Passive Micromixer with T Micromixer with Square Chamber Mixing Units (SAR)

Hani Attar
Faculty of Engineering
Zarqa University
Zarqa, Jordan
College of Engineering
University of Business and Technology
Jeddah, Saudi Arabia
Hattar@zu.edu.jo

Rahma S. Zekry
Department of Bioelectronics, Modern University of Technology and Information (MTI) University
Cairo, Egypt
rahma.91138@eng.mti.edu.eg

Mohanad A. Deif
Department of Artificial Intelligence, College of Information Technology, Misr University for Science & Technology (MUST)
6th of October City 12566, Egypt
Mohanad.Deif@must.edu.eg

Samer M. Sharfo
Department of Bioelectronics, Modern University of Technology and Information (MTI) University
Cairo, Egypt
samer.86027@eng.mti.edu.eg

Mohamed Hafez
Faculty of Engineering FEQS
INTI-IU-University
Nilai, Malaysia
mohdahmed.hafez@newinti.edu.my

Ahmad Solyman
School of Computing, Engineering and Built Environment, Glasgow
Caledonian University
Glasgow, UK
ahmed.solyman@gcu.ac.uk

***Abstract*—Microscale mixing methods are crucial in various disciplines, encompassing chemical reactions and biological investigations. The present study used simulation methodologies to investigate the operational efficiency of splitting recombination (SAR) micromixers. The study demonstrates that SAR micromixers offer a notable advantage in enhancing mixing efficiency. The advantage above is a consequence of the effective combination of splitting-recombination and chaotic advection processes within the micromixer architecture. An in-depth analysis of the micromixer's behavior demonstrates that its performance is supported by intricate fluid dynamics, which provide remarkably high mixing efficiency. It is worth noting that the micromixer exhibits its maximum mixing efficiency, which is roughly 99% when the Reynolds number (Re) is at or below 0.5. Nevertheless, it is seen that as the Reynolds number grows, there is a steady decrease in mixing efficiency. At a Reynolds number of 70, the measurement of mixing efficiency yields a value of 75%. However, when the Reynolds number is further increased to a range of 90-100, the efficiency decreases to its lowest value of approximately 60%. The results above highlight the exceptional mixing ability of the SAR micromixer, hence stressing its potential for various applications that demand improved mixing capabilities. The results emphasize the promise of SAR micromixers as a reliable solution for complex mixing processes in many applications, providing valuable insights that may contribute to future developments in microscale mixing technologies.**

Keywords—Micro-Fluidic, Micro-Mixer, Reynolds Number, Mixing Efficiency, Laminar Flow.

I. INTRODUCTION

Microfluidics pertains to devices and methodologies employed to control and manipulate fluid flows at length scales below a millimeter. The rapid development of microfluidic devices can be attributed to their extensive utilization in various scientific and engineering applications [1]. One of the crucial parts of a microfluidic system is the micromixer, which needs to be carefully planned in terms of its ease of production, practical uses, mixing performance, and integration. Combining fluid samples at a tiny scale can be challenging to prompt an appropriate reaction quickly. Turbulence, a phenomenon typically absent on a microscopic scale, governs the fundamental mixing mechanism. At the microscopic scale, mixing is constrained by the low Reynolds numbers. The two primary categories of micromixers are active and passive micromixers. Micromixers that are active need an outside energy source[2].

They have exceptional mixing capabilities, but because of the complexity of their fabrication, they also have drawbacks. Passive micromixers offer several advantages over their active counterparts, including easy fabrication, cost-effectiveness, seamless integration with microfluidic systems, the absence of intricate control components, and the elimination of supplementary power requirements[3]. Unlike active micromixers, passive ones don't necessitate external energy sources. The efficacy of passive micromixers in mixing is primarily determined by the channel configuration employed to induce fluid agitation or lamination, enhancing material interaction [4]. The channel shape largely determines how well passive micromixers perform. Hence, a comprehensive comprehension of the flow dynamics within the microchannel is imperative in constructing passive micromixers. Computational Fluid Dynamics (CFD) is a valuable approach for constructing efficient micromixers. Successful mixing in passive micromixers relies on the combined mechanisms of molecular diffusion and chaotic advection [5] and [6]. The investigation of fluid mixing in linear and intricate microchannels has been conducted through numerical simulations and practical experimentation [7]. The smart effect has been used to construct an in-plane passive micromixer to enhance mixing [8].

In microfluidics, researchers have explored chaotic micromixers featuring intersecting two-layer channels, showcasing rapid mixing capabilities even at low Reynolds numbers [9]. Investigations into T-type micromixers encompassed variations in channel diameters – fixed and variable – to assess their respective mixing efficiencies [10]. The mechanism of split and recombination (SAR) of flows has

emerged as a chaotic mixing strategy that remarkably enhances the interfacial area and, thus, elevates mixing performance across an extensive Reynolds number spectrum. Building upon SAR and chaotic advection principles, a serpentine laminar micromixer was developed, capitalizing on the strategic arrangement of "F"-shaped mixing units in two layers [11]. The influence of rotation on split and recombination mixing within micromixers has been a subject of investigation, leading to the development of three distinct types of SAR micromixers [12]. Passive micromixing exploiting fluid rotation has been demonstrated to induce fluid blending at low and high Reynolds numbers, resulting in an expanded region between the two fluids due to stretching and folding dynamics [13].

A passive micromixer, scrutinized experimentally and numerically, was developed based on intersecting fluid streams and asymmetric divisions. The study revealed that the unbalanced collision of these fluid streams, arising from differing mass flow rates in the sub-channels, perturbs and modifies the interface between them, thereby intensifying mixing dynamics [14]. Furthermore, a three-dimensional Split and Recombination (SR) based microreactor design has been proposed. The investigation highlights the substantial influence of the SR microreactor's geometric layout on chaotic advection and multi-laminar mixing phenomena [15]. Numerous other passive micromixers have harnessed the SAR process to create ultra-thin fluid stream layers [16], [17], demonstrating remarkable efficiency even at low Reynolds numbers. Research has also been conducted on a T-junction-based micromixer and serially interconnected mixing channel comprised of modules with distinct square, right-shifted, and left-shifted T-shaped cross sections [18].

The SAR-shaped micromixers are the most prevalent among all conceivable designs for micromixers and microreactors. Such micromixers are an essential component of practically every sophisticated micromixing apparatus, and when used alone, they perform admirably. Extensive explorations involving both experimental and numerical approaches have been carried out to investigate the flow dynamics and mixing patterns within these micromixers, spanning from references [19], [20], [21], [22], [23], [24], [25], [26], [27], [28], [29], [30], [31], [32], [33], [34], [35], [36], [37], [38], [39], [40], [41]. The study specifically delved into the blending of two fluids exhibiting akin thermophysical attributes, revealing the existence of six discernible flow regimes contingent upon the Reynolds number[42]. These regimes are delineated based on their respective ranges within Table 1.

TABLE 1:REYNODS NUMBER RANGE AND DESCRIBED THIS RANGE

NO.	The Range	Study(described)
1	0<Re<5.	steady stratified flow.
2	5< Re < 145.	steady symmetric vortex flow.
3	145< Re < 240.	steady asymmetric vortex flow.
4	240< Re < 400.	periodic flow.
5	400< Re < 600.	unsteady quasiperiodic flow.
6	Re > 600.	stochastic flow, laminar-turbulent transition.

Moreover, a significant portion of the research papers underscored a notable surge in mixing efficiency as the transition from symmetric to asymmetric flow regimes, commonly called the "engulfment regime"[43], occurred. [44]This transition, which occurs abruptly once the Reynolds number surpasses a specific critical value denoted as Recr, garners substantial attention. The heightened interest stems from the fact that within this regime, there is only a marginal increment in pressure drop across the mixing channel, yet a remarkable and substantial increase in mixing efficiency is achieved. Numerous variables affect the crucial Reynolds number's value[45].

A comprehensive investigation has been undertaken, encompassing four microfluidic mixers designed with square-wave microchannels inspired by compact disks (CDs). Both numerical simulations and practical experimentation were employed to scrutinize these mixers, focusing on their flow attributes and mixing capabilities. These mixers feature distinct numbers and arrangements of intake channels, contributing to a holistic understanding of their performance [46]. Employing a three-dimensional vortex micromixer that makes use of self-rotation effects[47] has been suggested. An experimental analysis investigated the device's fluid and mixing dynamics [48] [49]. They looked into a passive micromixer that improves mixing performance by allowing the fluid in the mixing chamber with the intake and outflow ports to circulate independently.

In summary, manipulating microchannel design can enhance mixing by increasing the interfacial area between fluid segments. Circular mixing chambers particularly demonstrate effective mixing performance. This study proposes passive micromixers leveraging microfluidic recirculation within circular and square mixing chambers to elevate mixing efficiency[50].

II. Micro-Mixer Design

Fig. 1 displays the dimensional representation of the SAR micromixer. The micromixer has a 6 mm overall length. The inlets and outlets' hydraulic diameter (Dh) is 0.133 mm, as are the channels' width and depth.

Water and ethanol were selected as the two working fluids for the mixing experiments. The fluid characteristics of water were measured at a temperature of 20°C. ethanol and water have densities of 789 and 998 kg/m3 and viscosities of 1.2×10^{-3} and 0.9×10^{-3} Pa s, respectively. The mixture of ethanol and water has a diffusion coefficient of 1.2×10^{-9}m2 /s. The study encompassed Reynolds numbers spanning from 0.5 to 100. This is how the Reynolds number is explained:

$$Re = \frac{\rho U Dh}{\mu} \quad (1)$$

Here, ρ represents fluid density, U signifies fluid velocity within the inlet channel, Dh denotes the hydraulic diameter of said channel, and μ characterizes the fluid's dynamic viscosity.

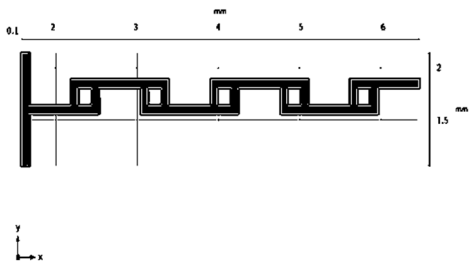

Fig. 1 . Schematics of the SAR micromixer with dimensions.

III. NUMERICAL SIMULATION

This study utilized the computational fluid dynamics (CFD) software COMSOL Multiphysics 6.0 to solve the governing equations. These governing equations, which include the Navier–Stokes equation, continuity equation, and species diffusion–convection equation, can be concisely expressed by the following equations, respectively:

$$\rho\left[\frac{\partial \mathrm{u}}{\partial \mathrm{t}} + (u.\nabla)\mathrm{u}\right] = -\nabla \mathrm{p} + \mathrm{u}\nabla^2 u \quad (2)$$

$$\nabla \mathrm{u} = 0 \quad (3)$$

$$\frac{\partial \mathrm{c}}{\partial \mathrm{t}} = \mathrm{D}\nabla^2 \mathrm{c} - \mathrm{u}\,.\nabla \mathrm{c} \quad (4)$$

In this context, u represents fluid velocity, ρ stands for fluid density, p signifies pressure, and μ characterizes the fluid's dynamic viscosity. Meanwhile, c and D denote the species' concentration and diffusion constant. Since studying this is stationary and does not depend on time, **∂c/ ∂t** and **∂u/∂t** are zero (0).

The boundary conditions implemented in this study were as follows: no-slip conditions were enforced at the walls of the channel, thereby maintaining uniform volume flow rates at both inlets. Furthermore, a zero-pressure boundary condition was imposed at the outlet. One of the inlets sustained a molar concentration of 1 mol/m³, while the other inlet featured a molar concentration of 0 mol/m³. Notably, the impact of gravity and its associated effects were deliberately excluded from consideration. To quantify the degree of mixing, the mixing index of the species at any specific cross-section within the mixing channel was computed employing the subsequent equations:

$$\sigma^2 = \frac{1}{\mathrm{N}}\sum_{i=1}^{n}(Ci - Cm)^2 \quad (5)$$

$$MI = 1 - \sqrt{\frac{\sigma^2}{\sigma^2 max}} \quad (6)$$

In this context, N represents the total number of sampling points within the cross-section. Ci denotes the molar concentration at the sampling point, whereas Cm signifies the optimal molar concentration for achieving complete fluid blending, which is 0.5. The variable σ corresponds to the standard deviation of molar concentration, while σ max indicates the maximum standard deviation recorded. The mixing index (MI) of the micromixer ranges from 0 (representing minimal mixing at 0%) to 1 (indicating complete mixing at 100%).

A series of simulations was conducted to investigate the micromixer's mixing efficiency. These simulations encompassed variations in inlet velocities and Reynolds numbers.

The SAR micromixer's mixing performance was evaluated through a Multiphysics simulation employing the commercial software COMSOL Multiphysics 6.0. The construction of the 3D fluid model was facilitated using the COMSOL 6.0 software, depicted in Figure 1. Inlet 1 maintained a molar concentration of 0 mol/m³, while inlet 2 contained a concentration of 1 mol/m³. The study encompassed a Reynolds number range spanning from 0.5 to 100. The micromixer's boundary conditions encompass uniform inlet velocities and zero static pressure at the outlets. The channel walls were subjected to no-slip boundary conditions.

IV. RESULT AND DISCUSSION

A. Simulation Result(mixing performance)

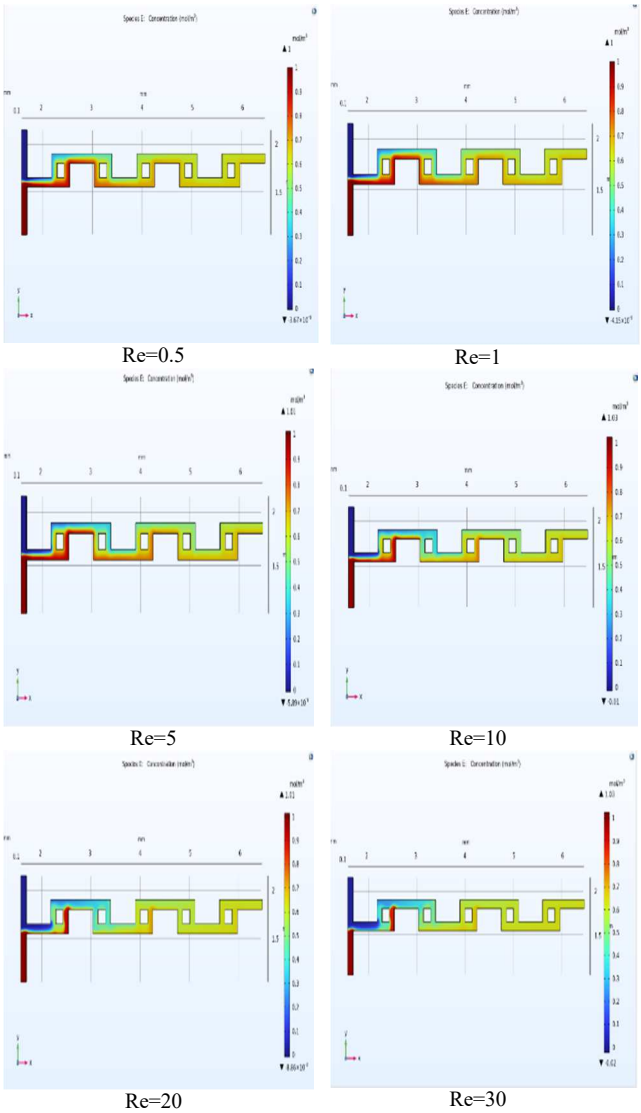

Re=0.5 Re=1

Re=5 Re=10

Re=20 Re=30

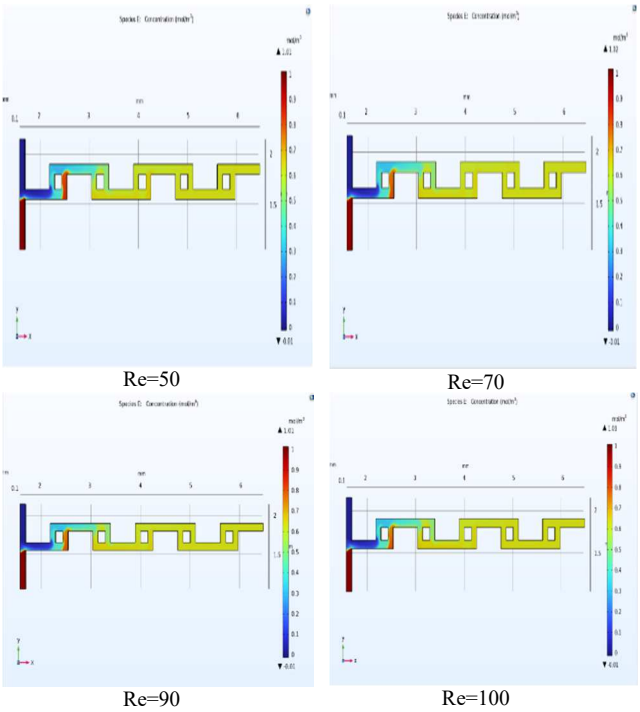

Fig.2. The comparison of the mixing performance of the SAR micromixer and at Re= 0.5 to 100, respectively.

Figure 2 illustrates a comparative analysis of the SAR micromixer's mixing performance across Reynolds numbers ranging from 0.5 to 100. The depiction highlights the progression of the SAR micromixer's mixing process, revealing distinct cross-sectional snapshots that elucidate the underlying mixing mechanisms. Vertically distributed concentration gradient contours are evident in the cross-sectional views, with fluid flow maintaining its laminar nature even as the mixing length increases. Notably, cross-sectional profiles resembling the letter "F" exhibit inverted concentration gradient contours, indicative of chaotic convection within these F-shaped mixing units.

These observations substantiate chaotic convection within the F-shaped mixing units, where the fluids undergo two turns as they traverse each unit. The resulting centrifugal force imparts changes to the fluid composition ratio. Subsequent marker-based experiments corroborate these findings, revealing that the F-shaped mixing units induce chaotic convection, enhancing mixing efficiency. Chaotic convection manifests as a complex motion pattern within microchannels. While initially adhering to simple physical laws, it transforms into a disorderly form when encountering F-bend angles that deviate significantly from anticipated regularity.

B. Simulation Result(velocity magnitude)

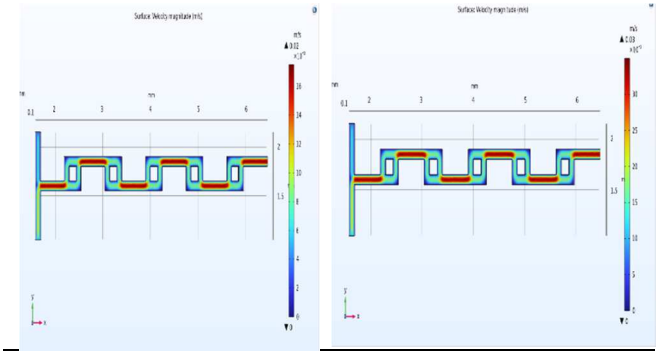

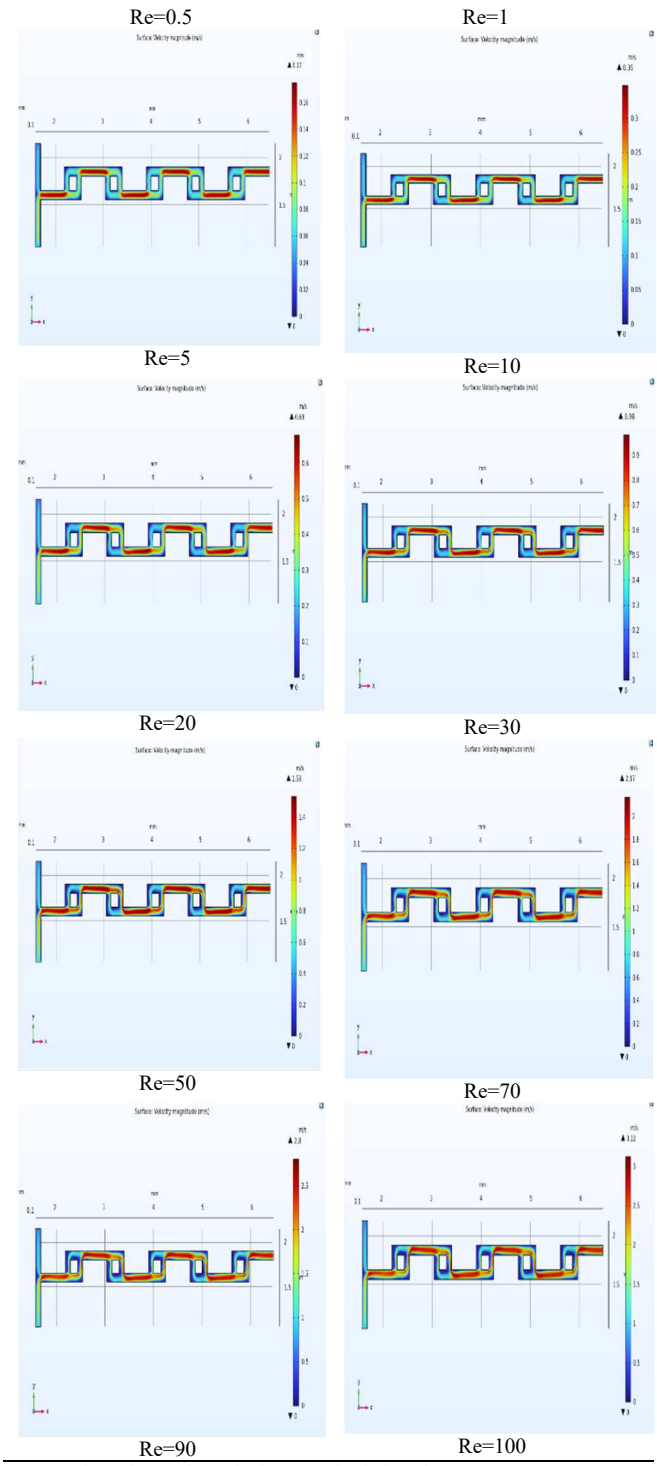

Fig.3 shows the Velocity magnitude in m/s at Re=0.5 to 100.

C. Simulation Result(contour pressure)

To comprehensively assess the SAR micromixer's performance, it becomes imperative to gauge its mixing efficiency. This evaluation systematically analyzes mixing efficiency across a spectrum of Reynolds numbers from 0.5 to 100 within a specific cross-sectional area at the micromixer's outlet. This assessment requires the extraction of concentrations from a designated set of sampling points (25 samples) situated at the outlet's cross-section. Subsequently, the mixing efficiency's evolution across the Reynolds number range can be ascertained by utilizing equations (5) and (6) and referencing Figure 2. The

concentration values obtained from the chosen samples are transferred to MATLAB software to execute this process. There, the mixing efficiency is determined by the varying Reynolds numbers (ranging from 0.5 to 100). This systematic approach enables a comprehensive understanding of how mixing efficiency evolves with changes in Reynolds number.

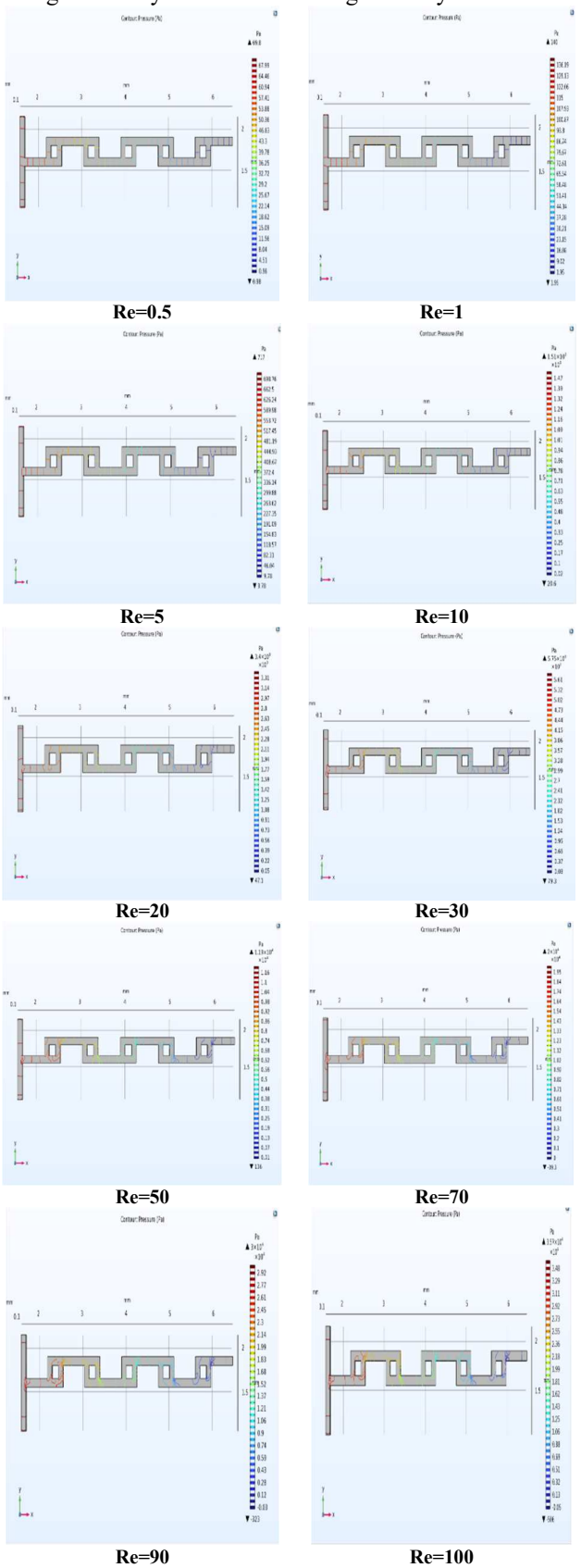

Fig.4 shows contour pressure in Pa at Re=0.5 to 100.

The relationship between mixing efficiency and Reynolds number is established based on the simulation outcomes illustrated in Figure 3. This characterization is achieved through the utilization of equations (5) and (6), and the subsequent representation of this relationship is generated using MATLAB software, resulting in the graph presented below:

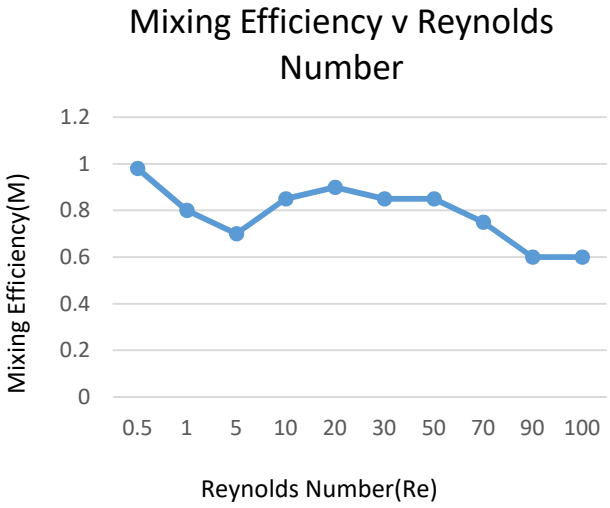

Fig.5.The development of the mixing efficiency with the increase of Reynolds numbers at the exits of the SAR micromixer.

Figure 5 illustrates the evolution of mixing efficiency concerning varying Reynolds numbers at the exits of the SAR micromixer. The mixing dynamics are primarily governed by molecular diffusion, influenced by residence time and the overall flow path length. A decrease in mixing efficiency occurs due to reduced residence time for diffusion. However, this trend shifts as Reynolds numbers surpass Re = 5. Here, introducing greater inertial forces disrupts the flow field, augmenting mixing. At Re = 90 and 100, the SAR micromixer displays its lowest mixing efficiency, measuring at 60%. In contrast, at Re = 0.5, the SAR micromixer attains its peak mixing efficiency at 99%, decreasing to 90% when Re = 20. These findings accentuate the SAR micromixer's exceptional mixing performance, outperforming other designs.

V. CONCLUSION

The numerical analysis of the mixing properties of the SAR micromixer was the focus of this study. COMSOL Multiphysics 6.0 was used to examine the mixing capabilities of SAR micromixers over a broad range of Reynolds numbers (Re=0.5, 1, 5, 10, 20, 30, 50, 70, and 100), using water and ethanol as the chosen working fluids. The SAR micromixer's effectiveness was investigated using splitting-recombination and chaotic convection methods.

Surprisingly, for lower Reynolds numbers (0.5–20), a rise in the Reynolds number was correlated with an astounding success of 99% mixing efficiency. In contrast, when the Reynolds number increased, the T micromixer's efficiency declined and eventually stabilized at roughly 60%. As a result, the SAR micromixer proved to have better mixing performance than previous micromixer setups. The potential of the SAR micromixer for advanced mixing applications was

increased by using splitting-recombination and chaotic convection mechanisms.

REFERENCES

[1] H. A. Stone, A. D. Stroock, and A. Ajdari, "Engineering flows in small devices: microfluidics toward a lab-on-a-chip," *Annu. Rev. Fluid Mech.*, vol. 36, pp. 381–411, 2004.

[2] M. A. Deif, M. A. A. Eldosoky, H. W. Gomma, A. M. El-Garhy, and A. S. Ell-Azab, "Adaptive neuro-fuzzy inference system controller technique for lower urinary tract system disorders," *J Clin Eng*, vol. 40, no. 3, pp. 135–143, 2015.

[3] Q. I. Ahmed, H. Attar, A. Amer, M. A. Deif, and A. A. A. Solyman, "Development of a Hybrid Support Vector Machine with Grey Wolf Optimization Algorithm for Detection of the Solar Power Plants Anomalies," *Systems*, vol. 11, no. 5, p. 237, 2023.

[4] A. Alam and K.-Y. Kim, "Mixing performance of a planar micromixer with circular chambers and crossing constriction channels," *Sens Actuators B Chem*, vol. 176, pp. 639–652, 2013.

[5] V. Hessel, H. Löwe, and F. Schönfeld, "Micromixers—a review on passive and active mixing principles," *Chem Eng Sci*, vol. 60, no. 8–9, pp. 2479–2501, 2005.

[6] S. S. Wang, Z. J. Jiao, X. Y. Huang, C. Yang, and N. T. Nguyen, "Acoustically induced bubbles in a microfluidic channel for mixing enhancement," *Microfluid Nanofluidics*, vol. 6, pp. 847–852, 2009.

[7] S. S. Das, S. D. Tilekar, S. S. Wangikar, and P. K. Patowari, "Numerical and experimental study of passive fluids mixing in micro-channels of different configurations," *Microsystem Technologies*, vol. 23, pp. 5977–5988, 2017.

[8] C.-C. Hong, J.-W. Choi, and C. H. Ahn, "A novel in-plane passive microfluidic mixer with modified Tesla structures," *Lab Chip*, vol. 4, no. 2, pp. 109–113, 2004.

[9] H. M. Xia, S. Y. M. Wan, C. Shu, and Y. T. Chew, "Chaotic micromixers using two-layer crossing channels to exhibit fast mixing at low Reynolds numbers," *Lab Chip*, vol. 5, no. 7, pp. 748–755, 2005.

[10] D. Gobby, P. Angeli, and A. Gavriilidis, "Mixing characteristics of T-type microfluidic mixers," *Journal of Micromechanics and microengineering*, vol. 11, no. 2, p. 126, 2001.

[11] D. S. Kim, S. H. Lee, T. H. Kwon, and C. H. Ahn, "A serpentine laminating micromixer combining splitting/recombination and advection," *Lab Chip*, vol. 5, no. 7, pp. 739–747, 2005.

[12] S. W. Lee and S. S. Lee, "Rotation effect in split and recombination micromixing," *Sens Actuators B Chem*, vol. 129, no. 1, pp. 364–371, 2008.

[13] S.-J. Park, J. K. Kim, J. Park, S. Chung, C. Chung, and J. K. Chang, "Rapid three-dimensional passive rotation micromixer using the breakup process," *Journal of micromechanics and microengineering*, vol. 14, no. 1, p. 6, 2003.

[14] M. A. Ansari, K.-Y. Kim, K. Anwar, and S. M. Kim, "A novel passive micromixer based on unbalanced splits and collisions of fluid streams," *Journal of micromechanics and microengineering*, vol. 20, no. 5, p. 055007, 2010.

[15] Y.-T. Chen, W.-F. Fang, Y.-C. Liu, and J.-T. Yang, "Analysis of chaos and FRET reaction in split-and-recombine microreactors," *Microfluid Nanofluidics*, vol. 11, pp. 339–352, 2011.

[16] F. Schönfeld, V. Hessel, and C. Hofmann, "An optimised split-and-recombine micro-mixer with uniform 'chaotic'mixing," *Lab Chip*, vol. 4, no. 1, pp. 65–69, 2004.

[17] H. Chen and J.-C. Meiners, "Topologic mixing on a microfluidic chip," *Appl Phys Lett*, vol. 84, no. 12, pp. 2193–2195, 2004.

[18] S.-W. Huang, C.-Y. Wu, B.-H. Lai, and Y.-C. Chien, "Fluid mixing in a swirl-inducing microchannel with square and T-shaped cross-sections," *Microsystem Technologies*, vol. 23, pp. 1971–1981, 2017.

[19] A. Fani, S. Camarri, and M. V. Salvetti, "Unsteady asymmetric engulfment regime in a T-mixer," *Physics of Fluids*, vol. 26, no. 7, 2014.

[20] C. Galletti, M. Roudgar, E. Brunazzi, and R. Mauri, "Effect of inlet conditions on the engulfment pattern in a T-shaped micro-mixer," *Chemical Engineering Journal*, vol. 185, pp. 300–313, 2012.

[21] A. Fani, S. Camarri, and M. V. Salvetti, "Investigation of the steady engulfment regime in a three-dimensional T-mixer," *Physics of Fluids*, vol. 25, no. 6, 2013.

[22] A. Soleymani, H. Yousefi, and I. Turunen, "Dimensionless number for identification of flow patterns inside a T-micromixer," *Chem Eng Sci*, vol. 63, no. 21, pp. 5291–5297, 2008.

[23] R. J. Poole, M. Alfateh, and A. P. Gauntlett, "Bifurcation in a T-channel junction: Effects of aspect ratio and shear-thinning," *Chem Eng Sci*, vol. 104, pp. 839–848, 2013.

[24] T. Andreussi, C. Galletti, R. Mauri, S. Camarri, and M. V. Salvetti, "Flow regimes in T-shaped micro-mixers," *Comput Chem Eng*, vol. 76, pp. 150–159, 2015.

[25] G. Orsi, M. Roudgar, E. Brunazzi, C. Galletti, and R. Mauri, "Water–ethanol mixing in T-shaped microdevices," *Chem Eng Sci*, vol. 95, pp. 174–183, 2013.

[26] A. S. Lobasov and A. V Minakov, "Analyzing mixing quality in a T-shaped micromixer for different fluids properties through numerical simulation," *Chemical Engineering and Processing-Process Intensification*, vol. 124, pp. 11–23, 2018.

[27] C. Galletti, E. Brunazzi, and R. Mauri, "Unsteady mixing of binary liquid mixtures with composition-dependent viscosity," *Chem Eng Sci*, vol. 164, pp. 333–343, 2017.

[28] W. Wang, S. Zhao, T. Shao, Y. Jin, and Y. Cheng, "Visualization of micro-scale mixing in miscible liquids using μ-LIF technique and drug nano-particle preparation in T-shaped micro-channels," *Chemical engineering journal*, vol. 192, pp. 252–261, 2012.

[29] C. Galletti, G. Arcolini, E. Brunazzi, and R. Mauri, "Mixing of binary fluids with composition-dependent viscosity in a T-shaped micro-device," *Chem Eng Sci*, vol. 123, pp. 300–310, 2015.

[30] A. S. Lobasov and A. A. Shebeleva, "Initial temperatures effect on the mixing efficiency and flow modes in T-shaped micromixer," in *Journal of Physics: Conference Series*, IOP Publishing, 2017, p. 022010.

[31] A. S. Lobasov, A. V Minakov, and V. Y. Rudyak, "Viscosity effect on the flow patterns in T-type micromixers," *Fluid dynamics*, vol. 51, pp. 381–388, 2016.

[32] A. Minakov, A. Yagodnitsyna, A. Lobasov, V. Rudyak, and A. Bilsky, "Study of fluid flow in micromixer with symmetrical and asymmetrical inlet conditions," *La Houille Blanche*, no. 5, pp. 12–21, 2013.

[33] A. Lobasov and A. Minakov, "Density effect on the mixing efficiency and flow modes in T-shaped micromixers," in *MATEC Web of Conferences*, EDP Sciences, 2017, p. 07002.

[34] A. Minakov, V. Rudyak, A. Dekterev, and A. Gavrilov, "Investigation of slip boundary conditions in the T-shaped microchannel," *Int J Heat Fluid Flow*, vol. 43, pp. 161–169, 2013.

[35] S. Dreher, N. Kockmann, and P. Woias, "Characterization of laminar transient flow regimes and mixing in T-shaped micromixers," *heat transfer engineering*, vol. 30, no. 1–2, pp. 91–100, 2009.

[36] D. Bothe, C. Stemich, and H.-J. Warnecke, "Fluid mixing in a T-shaped micro-mixer," *Chem Eng Sci*, vol. 61, no. 9, pp. 2950–2958, 2006.

[37] A. V Minakov, V. Y. Rudyak, A. A. Gavrilov, and A. A. Dekterev, "Mixing in a T-shaped micromixer at moderate Reynolds numbers," *Thermophysics and Aeromechanics*, vol. 19, pp. 385–395, 2012.

[38] C. Stemich, "Theoretische und numerische Untersuchung des Struomungsmischens in einem T-formigen Mikromischer," *Fakultät für Naturwissenschaften-Department Chemie*, 2006.

[39] C. Gobert, F. Schwertfirm, and M. Manhart, "Lagrangian scalar tracking for laminar micromixing at high Schmidt numbers," in *Fluids Engineering Division Summer Meeting*, 2006, pp. 1053–1062.

[40] M. Hoffmann, M. Schlüter, and N. Räbiger, "Experimental investigation of liquid–liquid mixing in T-shaped micro-mixers using μ-LIF and μ-PIV," *Chem Eng Sci*, vol. 61, no. 9, pp. 2968–2976, 2006.

[41] R. E. Hammam *et al.*, "Prediction of wear rates of UHMWPE bearing in hip joint prosthesis with support vector model and grey wolf optimization," *Wirel Commun Mob Comput*, vol. 2022, pp. 1–16, 2022.

[42] M. A. Deif, A. A. A. Solyman, and R. E. Hammam, "ARIMA Model Estimation Based on Genetic Algorithm for COVID-19 Mortality Rates," *Int J Inf Technol Decis Mak*, vol. 20, no. 6, pp. 1775–1798, 2021.

[43] A. Alqerem, H. Attar, W. Alomoush, and M. Deif, "The Ability of Ultra Wideband to Differentiate Between Hematoma and Tumor Occur in The Brain," in *2022 International Engineering Conference on Electrical, Energy, and Artificial Intelligence (EICEEAI)*, 2022, pp. 1–7.

[44] N. Baghdadi, A. S. Maklad, A. Malki, and M. A. Deif, "Reliable Sarcoidosis Detection Using Chest X-rays with EfficientNets and

Stain-Normalization Techniques," *Sensors*, vol. 22, no. 10, p. 3846, 2022.

[45] N. Baghdadi, A. S. Maklad, A. Malki, and M. A. Deif, "Reliable sarcoidosis detection using chest x-rays with efficientnets and stain-normalization techniques," *Sensors*, vol. 22, no. 10, p. 3846, 2022.

[46] J.-N. Kuo and Y.-S. Li, "Centrifuge-based micromixer with three-dimensional square-wave microchannel for blood plasma mixing," *Microsystem Technologies*, vol. 23, pp. 2343–2354, 2017.

[47] R. E. Hammam, A. A. A. Solyman, M. H. Alsharif, P. Uthansakul, and M. A. Deif, "Design of Biodegradable Mg Alloy for Abdominal Aortic Aneurysm Repair (AAAR) Using ANFIS Regression Model," *IEEE Access*, vol. 10, pp. 28579–28589, 2022.

[48] C.-H. Lin, C.-H. Tsai, and L.-M. Fu, "A rapid three-dimensional vortex micromixer utilizing self-rotation effects under low Reynolds number conditions," *Journal of Micromechanics and Microengineering*, vol. 15, no. 5, p. 935, 2005.

[49] Y.-C. Chung, Y.-L. Hsu, C.-P. Jen, M.-C. Lu, and Y.-C. Lin, "Design of passive mixers utilizing microfluidic self-circulation in the mixing chamber," *Lab Chip*, vol. 4, no. 1, pp. 70–77, 2004.

[50] E. M. O. Mokhtar and M. A. Deif, "Towards a Self-sustained House: Development of an Analytical Hierarchy Process System for Evaluating the Performance of Self-sustained Houses," *ENGINEERING JOURNAL*, vol. 2, no. 2, 2023.